Cell Death and Differentiation (2001) 8, 152–161

www.nature.com/cdd

# Zinc-mediated regulation of caspases activity: dose-dependent inhibition or activation of caspase-3 in the human Burkitt lymphoma B cells (Ramos)

**N Schrantz[1], M-T Auffredou[1], MF Bourgeade[1], L Besnault[1], G Leca[1] and A Vazquez*,[1]**

[1] INSERM U.131 and Association Claude Bernard, 32 rue des carnets, 92140 Clamart, France

* Corresponding author: A Vazquez, INSERM U.131, 32 rue des Carnets, 92140 Clamart, France. Tel: 33 1 41 28 80 04; Fax: 33 1 46 32 79 93; E-mail: vazquez@infobiogen.fr

Received 1.3.00; revised 22.8.00; accepted 30.8.00
Edited by SJ Martin

## Abstract

**Divalent cations, including Zinc and Manganese ions, are important modulators of cell activation. We investigated the ability of these two divalent cations to modulate apoptosis in human Burkitt lymphoma B cells line (Ramos). We found that Zinc (from 10 to 50 $\mu$M) inhibited Manganese-induced caspase-3 activation and apoptosis of Ramos cells. Higher concentration of Zinc (50 to 100 $\mu$M) did not prevent Manganese-mediated apoptosis but rather increased cell death among Ramos cells. This Zinc-mediated cell death was associated with apoptotic features such as cell shrinkage, the presence of phosphatidylserine residues on the outer leaflet of the cells, chromatin condensation, DNA fragmentation and decrease of mitochondrial transmembrane potential. Zinc-mediated apoptosis was associated with caspase-9 and caspase-3 activation as revealed by the appearance of active p35 fragment of caspase-9 and p19 and p17 of caspase-3 as well as *in vivo* cleavage of PARP and of a cell-permeable fluorogenic caspase-3 substrate (Phiphilux-$G_1D_2$). Both Zinc-mediated apoptosis and caspase-3 activation were prevented by the cell-permeable, broad-spectrum inhibitor of caspases (zVAD-fmk) or overexpression of bcl-2. In addition, we show that Zinc-induced loss of transmembrane mitochondrial potential is a caspase-independent event, since it is not modified by the presence of zVAD-fmk, which is inhibited by overexpression of bcl-2. These results indicate that depending on its concentration, Zinc can exert opposite effects on caspase-3 activation and apoptosis in human B lymphoma cells: concentrations below 50 $\mu$M inhibit caspase-3 activation and apoptosis whereas higher concentrations of Zinc activate a death pathway associated with apoptotic-like features and caspase-3 activation.** *Cell Death and Differentiation* (2001) **8,** 152–161.

**Keywords:** apoptosis; zinc; caspase; Burkitt lymphoma

**Abbreviations:** $Zn^{2+}$, Zinc ($ZnCl_2$); $Mn^{2+}$, Manganese ($MnCl_2$); PARP, poly(ADP-ribose) polymerase; zVAD-fmk, Z-Val-Ala-DL-Asp-fluoromethylketone; $\Delta\Psi m$, mitochondrial transmembrane potential; $DiOC_6(3)$, 3,3'dihexylocarbocyanine iodide; HE, Hydroethidine

## Introduction

Various cellular functions are influenced by essential trace-elements such as the divalent cations Zinc ($Zn^{2+}$) and Manganese ($Mn^{2+}$). The physiological concentrations of these cations are strictly controlled and divergence from normal levels are associated with various diseases.[1–6] For instance, $Zn^{2+}$ deficiency is mostly associated with increased apoptosis resulting in thymus atrophy, loss of splenocytes and lymphopenia, suggesting that this deficiency alters the apoptotic process involved in normal lymphopoiesis.[7–9] Nevertheless, $Zn^{2+}$-mediated regulation of apoptosis *in vivo* is probably more complex. Thus, patients with Down's Syndrome, have low plasma $Zn^{2+}$ levels and present both immature myeloid cells in peripheral blood and large numbers of apoptotic peripheral blood cells.[6,10] Several studies have shown that $Zn^{2+}$ supplementation in Down's Syndrome patients results both in the disappearance of peripheral myeloid precursor cells through an apoptotic process and the reduction of apoptotic peripheral blood cells.[6,10] These studies demonstrated that, *in vivo*, $Zn^{2+}$ can exert opposite effects on apoptosis, although the molecular basis of these different activities have not yet been elucidated. Pharmacological $Zn^{2+}$ supplementation is not only able to restore an impaired immune response but also improve normal immune function by raising the physiological $Zn^{2+}$ serum level of 8–12 $\mu$M about 10-fold to 100 $\mu$M.[11] Higher concentrations of extracellular $Zn^{2+}$ (500–1000 $\mu$M) have frequently been used to block apoptosis in a variety of systems. Surprisingly, lower and more physiological concentrations of $Zn^{2+}$ (80–200 $\mu$M) can induce partial death in thymocytes.[12]

Numerous metalloenzymes are $Zn^{2+}$-dependent and require $Zn^{2+}$ for their structure, catalytic activity or regulation.[9,10,13–16] $Zn^{2+}$ also regulates the activity of metalloproteins dependent on other cations. For example, $Zn^{2+}$ inhibits the activity of a $Ca^{2+}/Mg^{2+}$-dependent endonuclease involved in internucleosomal DNA fragmentation observed during apoptosis.[17] The average content of intracellular labile $Zn^{2+}$, as measured by zinquin (a membrane-permeant fluorophore specific for $Zn^{2+}$) was approximately 20 pmol/$10^6$ cells in leukemic lymphocytes.[18] When intracellular pool was increased under conditions that suppress apoptosis, most of the labile $Zn^{2+}$ appeared to be localized in the cytoplasm within membrane-enclosed vesicles. This may indicate that target molecules are

primarily cytoplasmic as caspases.[19] $Zn^{2+}$ directly inhibits the activity *in vitro* of various recombinant caspases including caspase-3, -6, -7 and -8.[20,21] These caspases are cysteine-related proteases, which are synthesized as inactive proenzymes and activated *in vivo* during most apoptotic processes. The proenzymes are activated by cleavage at particular aspartate sites: the cleavage products form dimers which are the active forms.[22] Some caspases, such as caspase-9, may activate other family members, and final activation may also result from autoprocessing as reported for caspase-3.[23,24] Caspase activation in a cell is followed by cleavage of numerous substrates and changes in the plasma membrane, mitochondria and the nucleus. More than 10 different caspases have been described and several reports indicate that caspase-3 is a major effector of nuclear apoptotic events.[25–29] We previously reported that $Mn^{2+}$, another divalent cation, can trigger apoptosis in human B cells and this apoptosis is associated with caspase-3 activation.[30] Therefore, to precise the role of divalent cations in the control of apoptosis, we evaluated the ability of $Zn^{2+}$ to modulate both apoptosis and caspase-3 activation induced by $Mn^{2+}$.

We found that $Zn^{2+}$ exerts opposite effects on caspase-3 activation and apoptosis of Ramos human B lymphoma. At concentrations up to 50 $\mu$M, $Zn^{2+}$ inhibits the loss of mitochondrial membrane potential ($\Delta\Psi$m), and the activation of both caspase-9 and caspase-3 associated with apoptosis induced by $Mn^{2+}$. In contrast, no such inhibition of $Mn^{2+}$-mediated apoptosis was observed with higher concentrations of $Zn^{2+}$. Moreover, when used at concentrations of 60–100 $\mu$M, $Zn^{2+}$ activated a death pathway associated with caspase-9 and caspase-3 activation and apoptotic-like features which was inhibited in the presence of the caspase inhibitor zVAD-fmk or by overexpression of the Bcl-2 protein.

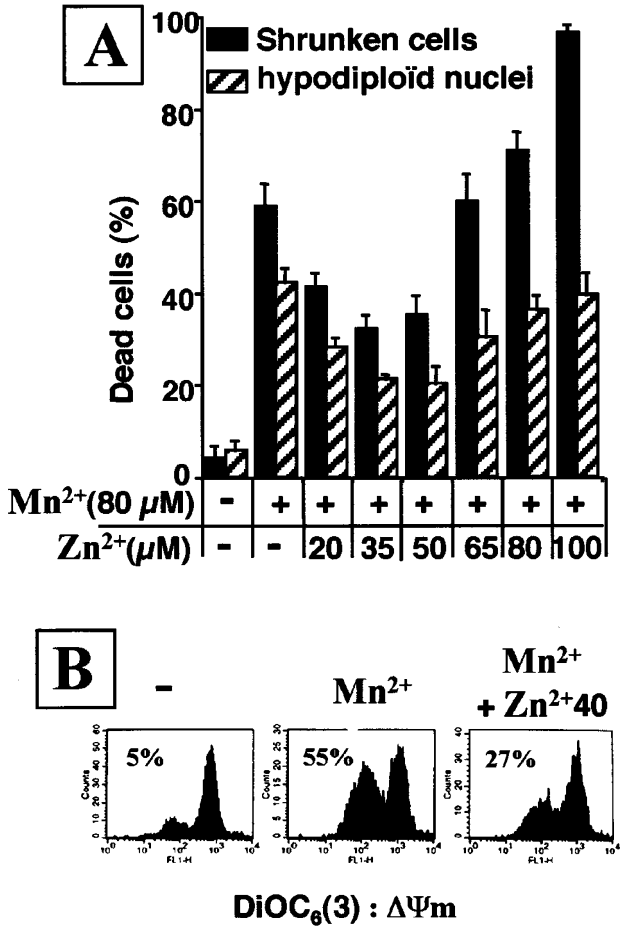


**Figure 1** Dual effects of $Zn^{2+}$ on $Mn^{2+}$-induced apoptosis. Ramos cells were cultured for 48 h without (–) or with $Mn^{2+}$ (80 $\mu$M) and various concentrations of $Zn^{2+}$. (**A**) Cell viability was assessed by flow cytometry. Shrunken cells having relatively high side-scatter (SSC) and low forward-scatter (FSC) properties were enumerated as a percentage of the total population. Cell nuclei were stained with PI and the hypodiploïd DNA peak corresponding to apoptotic nuclei was quantified. (**B**) Ramos cells were cultured for 48 h without (–) or with $Mn^{2+}$ (80 $\mu$M) in the absence ($Mn^{2+}$) or the presence of $Zn^{2+}$ (40 $\mu$M) ($Mn^{2+}$+$Zn^{2+}$40) and then stained with $DiOC_6(3)$ for analysis of mitochondrial transmembrane potential dissipation. One out of three similar experiments is shown

## Results

### Dual effect of $Zn^{2+}$ on $Mn^{2+}$-mediated apoptosis

We previously reported that human Burkitt lymphoma B cell lines, such as Ramos cells, were sensitive to $Mn^{2+}$-mediated apoptosis and that this apoptosis was associated with caspase-3 activation.[30] Several groups have reported that $Zn^{2+}$ inhibits caspase-3 activity and apoptosis.[20,21,31] We first studied the effect of various doses of $Zn^{2+}$ on $Mn^{2+}$-induced death of Ramos cells. Apoptosis was followed by measuring cell shrinkage or chromatin condensation evidenced by the appearance of hypodiploid nuclei. $Zn^{2+}$ at doses from 20 to 50 $\mu$M significantly decreased the apoptosis of Ramos cells observed in the presence of 80 $\mu$M $Mn^{2+}$ (Figure 1A). We next investigated which steps of the $Mn^{2+}$-induced apoptotic cascade were sensitive to the protective doses of $Zn^{2+}$. For this, we first tested the ability of $Zn^{2+}$ (40 $\mu$M) to interfere with the loss of mitochondrial membrane potential ($\Delta\Psi$m) induced by apoptotic concentrations of $Mn^{2+}$ (80 $\mu$M). There was a significant inhibition (52%) of the $Mn^{2+}$-mediated loss of $\Delta\Psi$m as quantified by staining with $DiOC_6(3)$ (Figure 1B). Thus, this protective effect of $Zn^{2+}$ is manifest at an early stage, at the mitochondrial level. The mechanism of this effect remains to be more precisely characterized. We then verified whether activation of downstream caspases such as caspase 9 and 3 were also inhibited by 40 $\mu$M $Zn^{2+}$ (Figure 2). The protective effect of $Zn^{2+}$ was associated with inhibition of $Mn^{2+}$-induced activation of caspase-9 (assessed as the production of active cleaved 37 fragment of caspase-9: Figure 2A) and caspase-3 (assessed as the production of active cleaved p19 and p17 fragments of caspase-3 or cleavage of the caspase-3 substrate PARP from the 110 kDa form to the 83 kDa fragment) in intact cells (Figure 2B). No protective effect was observed with higher doses of $Zn^{2+}$. In the presence of 65 $\mu$M $Zn^{2+}$, the cell death assessed by cell shrinkage, was equivalent to that observed with $Mn^{2+}$ alone (59% *vs* 58%). Higher concentrations of $Zn^{2+}$ (80 and 100 $\mu$M) increased the

percentage of cells dying (72 and 95% respectively) (Figure 1A). This dual effect of $Zn^{2+}$ was also observed on $Mn^{2+}$-mediated chromatin condensation, although to a lesser extend (Figure 1A). To verify that $Zn^{2+}$ was able to influence the viability of Ramos cells directly, we activated these cells with a series of doses of $Zn^{2+}$ and assessed cell shrinkage after 24 h of culture. Doses of 20 and 35 $\mu$M of $Zn^{2+}$ that counteracted the apoptotic effect of $Mn^{2+}$ (Figures 1 and 2) did not modify the viability of Ramos cells as indicated by cell shrinkage. Higher concentrations ($>50$ $\mu$M) of $Zn^{2+}$ increased cell shrinkage with maximal effect at 80 $\mu$M $Zn^{2+}$ (data not shown). Thus, depending on final concentration used, $Zn^{2+}$ exhibited opposite effects on the viability of Ramos cells. Doses up to 50 $\mu$M $Zn^{2+}$ did not promote Ramos cell death but protected the cells from $Mn^{2+}$-induced-apoptosis and -caspase-3 activation. In contrast, doses above 50 $\mu$M $Zn^{2+}$ directly induced Ramos cell death.

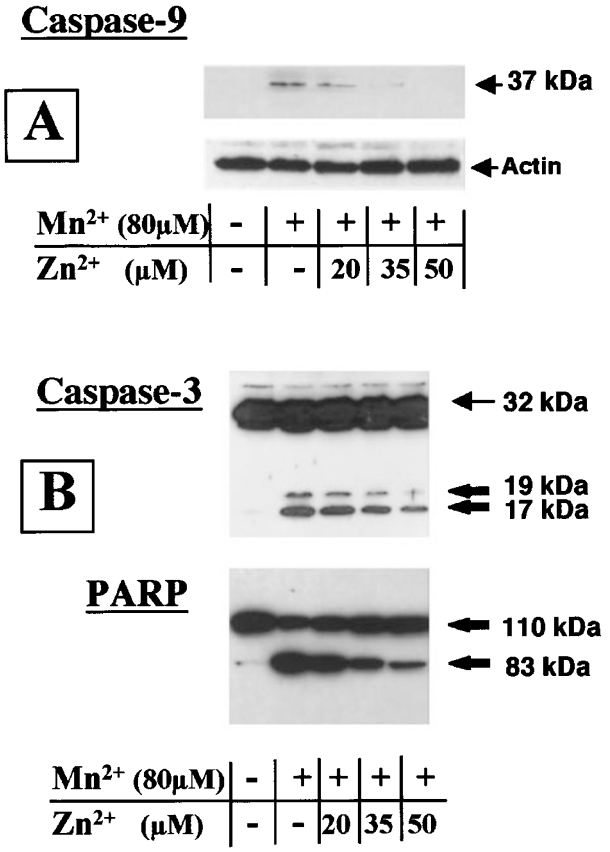


**Figure 2** $Zn^{2+}$-mediated inhibition of $Mn^{2+}$-induced apoptosis is associated with inhibition of caspase-9 and caspase-3 processing and activity. Ramos were cultured for 48 h in the absence (−) or in the presence of $Mn^{2+}$ (80 $\mu$M) and various concentrations of $Zn^{2+}$. (**A**) The amounts of p37 active subunit of caspase-9 and (B) p32 proform and p19 and p17 subunits of caspase-3 were analyzed by Western blotting with specific anti-cleaved caspase-9 and anti-caspase-3 antibodies respectively. (**B**) PARP cleavage was analyzed by Western blotting with an anti-PARP antibody

## Zinc-mediated cell death is associated with apoptotic phenomena

We next analyzed the features of $Zn^{2+}$-treated Ramos cells and in particular studied cytoplasmic and nuclear events (Figure 3). $Zn^{2+}$ at a final concentration of 60 $\mu$M induced cell shrinkage (52% *vs* 9% in control cells after 24 h of stimulation) as assessed by cell dot-blot light scatter profiles and flow cytometry (Figure 3A). Cell shrinkage correlated with cell viability, tested by trypan blue exclusion (data not shown). This cell shrinkage was also correlated with the presence of phosphatidylserine residues detected by Annexin V in these cells (57% *vs* 11.7% in control after 24 h of stimulation) (Figure 3B). Importantly, we consistently observed that, in

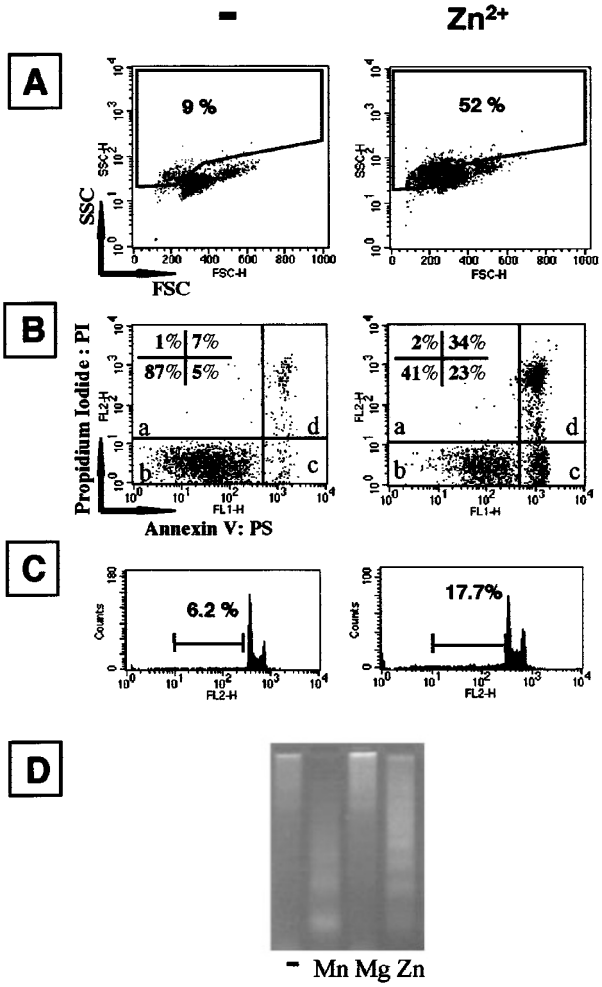


**Figure 3** Characterization of $Zn^{2+}$-mediated cell death. Cells were cultured for 24 h without (−) or with 60 $\mu$M $Zn^{2+}$ and studied for features of apoptosis. (**A**) Shrunken cells having relatively high side-scatter (SSC) and low forward-scatter (FSC) properties were enumerated as a percentage of the total population. (**B**) Cells were stained with Annexin-V-FITC and propidium iodide. Cells with phosphatidylserine residues on the outer leaflet without loss of cell integrity $PS^+/PI^-$ (c) were considered as apoptotic cells whereas $PS^+/PI^+$ (d) and $PS^-/PI^-$ (b) were considered as necrotic and viable cells respectively. (**C**) Cell nuclei were stained with PI and the hypodiploïd DNA peak corresponding to apoptotic nuclei was quantified. (**D**) DNA fragments from cells activated for 24 h without (−) or with 60 $\mu$M $Zn^{2+}$, 80 $\mu$M $Mn^{2+}$ or 100 $\mu$M $Mg^{2+}$ were analyzed as described in Materials and Methods

addition to necrotic cells ($PS^+/PI^+$), a significant number of cells had phosphatidylserine residues on the outer leaflet without loss of cell membrane integrity ($PS^+/PI^-$ cells: 22.3% *vs* 5% in control cells after 24 h treatment with $Zn^{2+}$). This morphological feature is typically associated with apoptotic death. Interestingly, in contrast to $Mn^{2+}$ which induced maximum apoptosis after 48 h of stimulation, the number of apoptotic cells ($PS^+/PI^-$) observed with $Zn^{2+}$ (60 $\mu$M) was maximum at 24 h whereas most of the dead cells observed at 48 h were necrotic (data not shown). $Zn^{2+}$-mediated cell death was also associated with chromatin condensation evidenced by the presence, after PI staining, of hypodiploid nuclei (17.7% *vs* 6.2% in control non activated cells) (Figure 3C). Moreover, DNA extracted from 24 h $Zn^{2+}$-activated cells exhibited also orderly fragmentation resulting in the appearance of a ladder-like cleavage pattern after electrophoresis (Figure 3D). This DNA fragmentation was similar to that observed in cells treated with 80 $\mu$M $Mn^{2+}$, whereas DNA extracted from cells treated with 100 $\mu$M $Mg^{2+}$, which did not exhibit cell mortality features, was similar to DNA from control cells. These results showed that 60 $\mu$M $Zn^{2+}$ induced substantial cell death of Ramos cells, and that this cell death, at least in an important fraction of these cells, was associated with phosphatidylserine expression on the outer leaflet of the cells without loss of cell membrane integrity, chromatin condensation and DNA fragmentation, all typical of apoptotis. Nevertheless, we did not observe nuclear fragmentation in $Zn^{2+}$-treated Ramos cells whereas similar activation with $Mn^{2+}$ promoted substantial fragmentation of Ramos cell nuclei (data not shown and [30]).

## $Zn^{2+}$-induced caspase-3 activation in Ramos cells is inhibited by the caspase inhibitor zVAD-fmk

We therefore investigated whether high doses of $Zn^{2+}$ (60 $\mu$M) stimulated caspase-3 activation. We used Western blotting to follow the appearance of cleaved active fragments of caspase-3 and quantified caspase-3 activation by monitoring the cleavage *in vivo* of both the natural substrate PARP and a synthetic substrate containing the caspase 3 target sequence GDEVDG (Phiphilux $G_1D_2$) (Figure 4). Sixty $\mu$M $Zn^{2+}$ induced the processing of caspase-3 proform into the active fragments p19 and p17. This caspase-3 activation was assayed by following the cleavage *in vivo* of PARP from the 110 kDa form to the 83 kDa fragment (Figure 4A). Proteolytic processing of caspase-3 and of the caspase-3 substrate PARP can occur during cell lysis through release of activated proteases, like granzyme B in T lymphocytes, able to cleave and activate caspase-3 *in vitro*.[32] We verified that $Zn^{2+}$ could also activate caspase-3 in intact cells using a cell-permeable fluorogenic caspase-3 substrate containing the sequence GDEVDG (Figure 4B). We next investigated whether inhibition of caspase activity with a broad spectrum inhibitor of caspase (zVAD-fmk) influenced $Zn^{2+}$-induced caspase-3 activation in Ramos cells. One hundred $\mu$M zVAD-fmk completely inhibited the appearance of the active cleaved fragments of caspase-3 and cleavage of PARP (Figure 4A). zVAD-fmk also prevented $Zn^{2+}$-mediated cleavage of the fluorogenic substrate Phiphilux-$G_1D_2$ in intact cells (36% in $Zn^{2+}$-activated cells *vs* 21% in $Zn^{2+}$-activated cells in the presence of zVAD-fmk and 24% in control cells) (Figure 4B). This zVAD-fmk-mediated inhibition of caspase-3 was specifically associated with prevention of $Zn^{2+}$-induced apoptosis: both $Zn^{2+}$-mediated chromatin condensation (18% hypodiploid nuclei in cells stimulated with 60 $\mu$M $Zn^{2+}$ *vs* 6% in cells activated with 60 $\mu$M of $Zn^{2+}$ in the presence of zVAD-fmk and 9% in control cells) and the appearance of $PS^+/PI^-$ cells (26% *vs* 9% in the presence of zVAD-fmk and 8% in control cells) were prevented by zVAD-fmk. In contrast, $Zn^{2+}$-induced necrosis observed after 24 h (25% $PS^+/PI^+$ *vs* 22% in the presence of zVAD and 7% in control cells respectively) was not significantly modified (Figure 4A). These results demonstrate that inhibition of caspase activity by zVAD-fmk abolished $Zn^{2+}$-mediated caspase-3 activation and the apoptotic features associated with cell death, indicating that $Zn^{2+}$ can promote caspase-3 activation in a caspase-dependent manner. We therefore investigated the ability of Zn to activate other caspases,

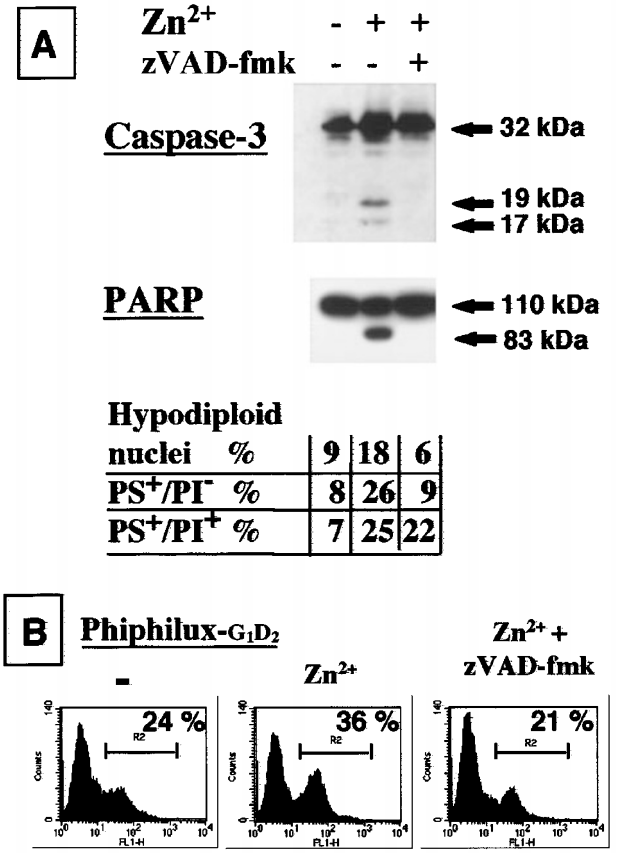


**Figure 4** effect of zVAD-fmk on $Zn^{2+}$-mediated-caspase-3 processing and apoptosis. Ramos cells were cultured in the presence of 60 $\mu$M $Zn^{2+}$ without (−) or with (+) 100 $\mu$M zVAD-fmk. (**A**) The amounts of 32 kDa proform and p19 and p17 subunits of caspase-3 were determined after 8 h by Western blotting. PARP cleavage was analyzed by Western blotting with a specific anti-PARP antibody. In parallel experiments various features of apoptosis were analyzed in control cells or cells activated or not for 24 h with 60 $\mu$M $Zn^{2+}$: percentage of $PS^+/PI^-$ or $PS^+/PI^+$ cells and hypodiploid nuclei. (**B**) The cleavage of Phiphilux-G1D2 was used to monitor caspase-3 activity in intact cells as described in Materials and Methods

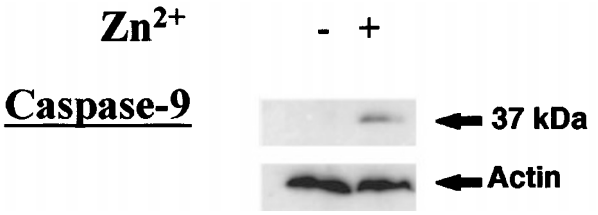


**Figure 5** $Zn^{2+}$-mediated-caspase-9 processing. Ramos cells were cultured in the absence (−) or the presence of 60 $\mu$M $Zn^{2+}$ (+) for 8 h. The amount of active cleaved caspase-9 (p37) was determined by Western blotting using a specific anti-p37 caspase-9 Ab. The amount of protein loaded in each lane was assessed by re hybridization of the filter with an Ab specific for human actin

including caspase-9, responsible for the cleavage and activation of caspase-3. Indeed, $Zn^{2+}$ (60 $\mu$M) induced the processing of the caspase-9 proform into the active fragment p37 (Figure 5).

### Overexpression of bcl-2 is sufficient to inhibit $Zn^{2+}$-induced caspase-3 activation

The bcl-2 protein is a potent inhibitor of both apoptosis and caspase-3 activation in diverse cells. Overexpression of bcl-2 counteracts apoptosis of human lymphoma B cells induced by $Mn^{2+}$.[30] We therefore studied whether overexpression of bcl-2 protein in Ramos cells modified the sensitivity of these cells to $Zn^{2+}$-induced caspase-3 activation and cell death. We first isolated a subclone of Ramos cells transfected with the human *bcl-2* gene (Ramos-bcl-2) and checked that the clone overproduced the protein bcl-2.[30] Ramos and Ramos-bcl-2 cells were activated with 100 $\mu$M $Zn^{2+}$ and caspase-3 activation and cell shrinkage were analyzed (Figure 6). Overexpression of bcl-2 prevented $Zn^{2+}$-mediated caspase-3 activation as indicated by the lack of production of p19 and p17 fragments and *in vivo* cleavage of PARP in Ramos-bcl2 cells as compared to Ramos. Caspase-3 activation was not observed in the presence of higher concentrations of $Zn^{2+}$ (data not shown). In parallel experiments, we studied the effect of bcl-2 overexpression on nuclear (chromatin condensation) and cell morphology ($PS^+/PI^-$ phenotype expression) following 100 $\mu$M $Zn^{2+}$ stimulation. $Zn^{2+}$-mediated chromatin condensation (22% *vs* 4% hypodiploid nuclei in $Zn^{2+}$-activated Ramos and Ramos-bcl-2 respect-ively) and $PS^+/PI^-$ phenotype expression (20% *vs* 1% $PS^+/PI^-$ cells in $Zn^{2+}$-activated Ramos and Ramos-bcl-2 respectively) were prevented by overexpression of bcl-2 (Figure 6B). Thus, overexpression of bcl-2 can prevent $Zn^{2+}$-mediated caspase-3 activation and apoptosis.

### $Zn^{2+}$-induced mitochondrial transmembrane potential ($\Delta\Psi$m) loss is caspase-independent

To precise the cascade of events promoted by $Zn^{2+}$ and leading to caspase-3 activation, we next measured, by staining with $DiOC_6(3)$ and HE, the loss of mitochondrial membrane potential ($\Delta\Psi$m) which is an early and

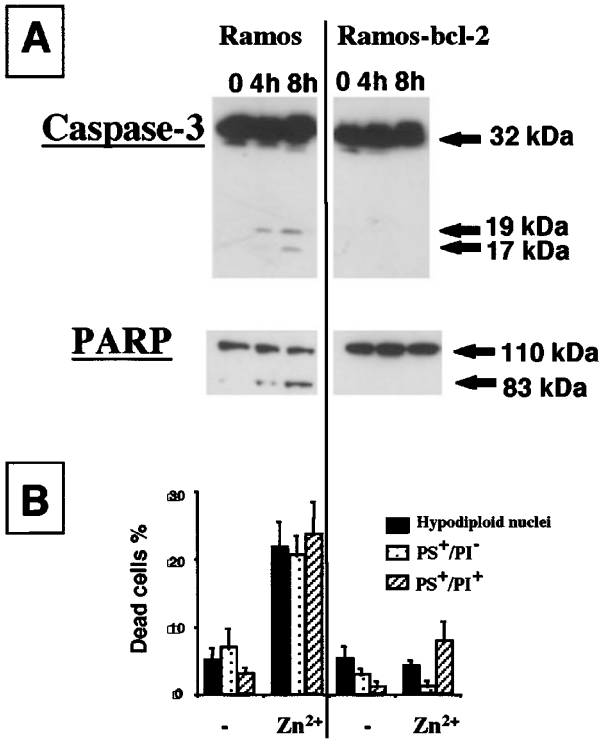


**Figure 6** Bcl-2 overexpression protects cells from $Zn^{2+}$-induced caspase-3 activation. Ramos and Ramos-bcl-2 cells were stimulated with 100 $\mu$M $Zn^{2+}$ for various periods of time. (**A**) p32 proform, p19 and p17 subunits of caspase-3 and cleavage of PARP were analyzed by Western blotting with specific anti-antibodies. (**B**) Various features of apoptosis were analyzed in parallel experiments in control cells or cells activated for 24 h with 100 $\mu$M $Zn^{2+}$: the percentages of $PS^+/PI^-$ and $PS^+/PI^+$ cells and hypodiploid nuclei were enumerated as previously described

irreversible step in apoptotic process and the generation of superoxide anions respectively.[33] $Zn^{2+}$ at 60 $\mu$M significantly increases the percentage of cells with low $\Delta\Psi$m (39% *vs* 22% in control, cells) (Figure 7A) and ethydium positive cells (38% *vs* 19% in control cells) (Figure 7B). When $Zn^{2+}$-mediated cell shrinkage was inhibited with different concentrations of zVAD-fmk, only superoxide anions production was reduced whereas the percentage of cells exhibiting a low $\Delta\Psi$m remains similar to that observed in cells activated with $Zn^{2+}$ in the absence of zVAD-fmk (Figure 7C). These data indicate that $Zn^{2+}$ can promote mitochondrial modification associated to apoptosis, such as loss of $\Delta\Psi$m, in a caspase-independent manner. In addition, we show that this loss of mitochondrial membrane potential is regulated by bcl-2, since overexpression of bcl-2 strongly inhibited loss of $\Delta\Psi$m observed with 100 $\mu$M $Zn^{2+}$ (Figure 7D) whereas $\Delta\Psi$m decrease obtained with 60 $\mu$M $Zn^{2+}$ was completely abrogated (data not shown).

## Discussion

In this report, we show that the ability of $Zn^{2+}$ to modulate apoptosis in the human Burkitt cell line Ramos is a complex

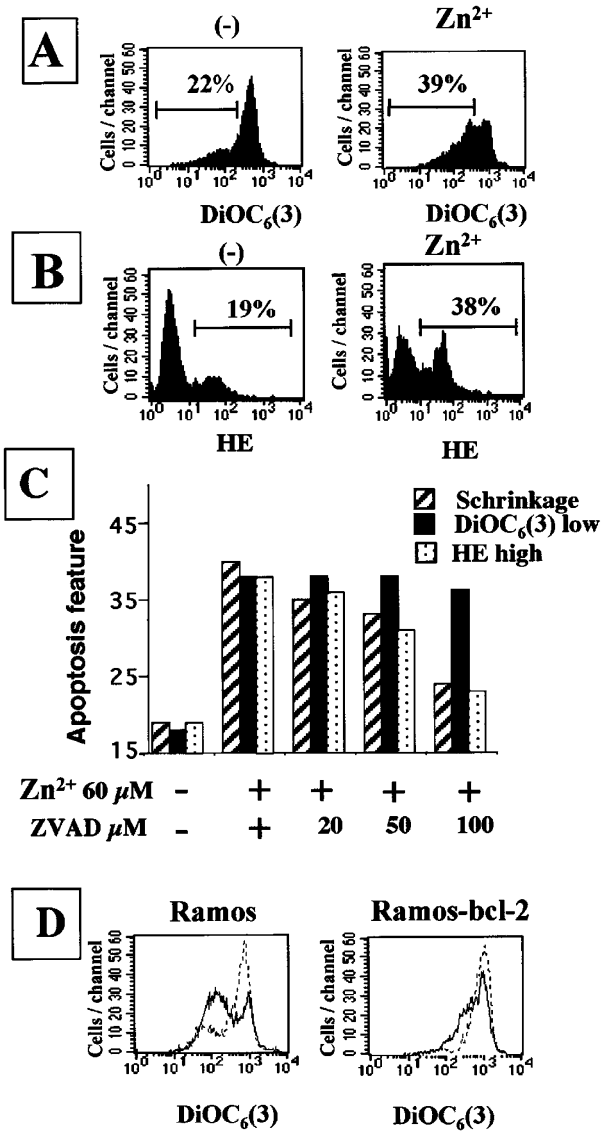


**Figure 7** Effect of ZVAD-fmk on $Zn^{2+}$-mediated mitochondrial transmembrane potential dissipation and superoxide anions production. Ramos cells were cultured in the absence or in the presence of 60 $\mu$M $Zn^{2+}$ for 8 h and then stained for $DiOC_6(3)$ (**A**) and HE (**B**) for analysis of mitochondrial transmembrane potential dissipation and superoxide anions production respectively. (**C**) Cells were cultured without or with 60 $\mu$M $Zn^{2+}$ and various concentrations of ZVAD-fmk for 8 h and analyzed for cell shrinkage, loss of mitochondrial transmembrane potential and production of superoxyde anions. The number of each cell population was enumerated as a percentage of the total population. Ramos and Ramos-bcl-2 cells were cultured without (broken line) or with (continuous line) 100 $\mu$M $Zn^{2+}$ for 12 h and then stained for $DiOC_6(3)$ for analysis of mitochondrial transmembrane potential dissipation

process which depends on the dose. We observed that concentrations of $Zn^{2+}$ above 50 $\mu$M activated caspase-3 in intact cells. This activation was evidenced by *in vivo* cleavage of the caspase-3 substrate PARP. To rule out a possible post-lytic, non-specific activation of caspase-3 *in vitro* as reported for PHA-activated T cells,[32] we verified that $Zn^{2+}$ could directly promote the cleavage in intact cells of a cell permeable fluorogenic caspase-3-like substrate containing the sequence GDEVDG (Phiphilux $G_1D_2$). These experiments showed that 60 $\mu$M $Zn^{2+}$ induced *in vivo* activation of caspases and cleavage of PARP and the sequence GDEVDG. The direct involvement of caspase-3 activation during this process was evidenced by the production in $Zn^{2+}$-activated Ramos cells of cleaved forms p19 and p17 recognized with a specific-caspase-3 antibody. In untreated control cells only the p32 proform of caspase-3 was detected. Although we can not exclude that other caspases able to cleave PARP or the sequence DEVD, such as caspase-2 or 7, could also be responsible for the caspase activity detected in $Zn^{2+}$-activated cells, our data provide for the first time evidence that $Zn^{2+}$ promotes a process leading to activation of caspase-3 in intact Burkitt cells.

It has recently been proposed that the caspase-3 proform can be cleaved into active forms by caspase-9 activated by a molecular complex including Apaf1 and cytochrome *c*.[34] In our experimental conditions, the large caspase inhibitor zVAD-fmk not only prevented cleavage of caspase-3 substrates but also prevented the appearance of the cleaved fragments p19 and p17 of caspase-3. Thus, $Zn^{2+}$-mediated caspase-3 activation appears to be dependent on the activation of upstream regulatory caspases. Indeed, caspase-9, which is the caspase responsible for direct cleavage and therefore activation of caspase-3, is also activated in the presence of apoptotic doses of $Zn^{2+}$.

Implication of upstream mitochondrial events during $Zn^{2+}$-induced caspase-3 activation is emphasized by the observation that this activation is (i) associated with loss of mitochondrial membrane potential and (ii) prevented by overexpression of the protooncogene bcl-2, which is thought to be a major regulator of the mitochondrial permeability transition pores governing the release of apoptotis regulators such as cytochrome *c*, AIF and caspase-9 itself.[34–36] Furthermore, we show that zVAD-fmk does not prevent $Zn^{2+}$-mediated loss of $\Delta\Psi m$ showing that the mitochondrial membrane potential dissipation induced by $Zn^{2+}$ is not a consequence of a direct effect of caspase activity. These data strongly suggest that the pathway leading to caspase-3 activation by $Zn^{2+}$ involves both caspase-dependent and -independent steps (Figure 8). In addition, this apoptotic pathway does not require protein synthesis since apoptosis triggered by $Zn^{2+}$ was not inhibited in the presence of cycloheximide (data not shown).

Interestingly, lower doses of $Zn^{2+}$ (below 50 $\mu$M) did not activate caspase-3 but on the contrary inhibited both apoptosis and caspase-3 activation promoted in Burkitt B cells by the divalent cation $Mn^{2+}$. These observations fit well with the $Zn^{2+}$-mediated inhibition of various caspases, including caspase-3 and caspase-6, previously reported by other groups.[21,22,31] In our experimental conditions, $Zn^{2+}$-mediated inhibition of $Mn^{2+}$-induced caspase-3 activation was associated with decrease in the amounts of both p19 and p17, the active fragments of caspase-3. As cleavage of the p19 form to the 17 kDa fragment is dependent on the autocatalytic activity of caspase-3,[23,37] it is possible that $Zn^{2+}$-mediated inhibition of PARP cleavage is associated with a decrease in the production of the active p19 fragment. This down-regulation of active caspase-3 fragments expression by

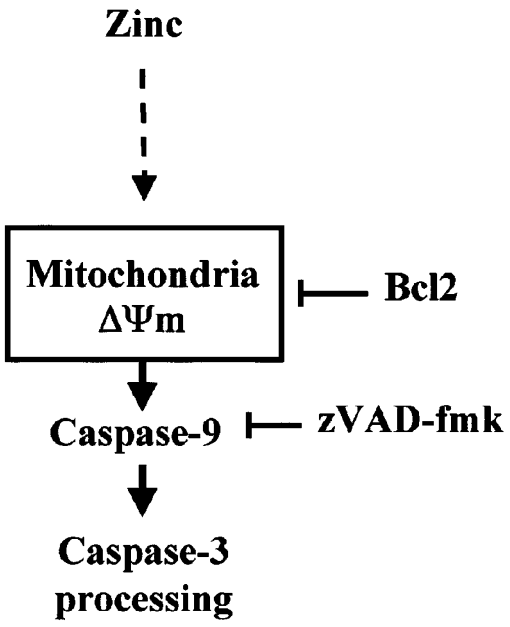


**Figure 8** Proposed model for Zn-mediated caspase-3 activation. Upon 60 $\mu$M $Zn^{2+}$ stimulation, $\Delta\Psi$m loss, sensitive to bcl-2, was promoted in a caspase-independent manner. Subsequent events, including caspase-9 activation, sensitive to the large caspase inhibitor zVAD-fmk, lead to activation of the caspase-3

$Zn^{2+}$ could be achieved in two different ways: $Zn^{2+}$ may inhibit some upstream events leading to $Mn^{2+}$-mediated caspase-3 activation and/or may upregulate the degradation of active caspase-3 fragments. Indeed, we observed that $Zn^{2+}$ could interfere with upstream events: it both prevented the loss of the mitochondrial membrane potential ($\Delta\Psi$m) and inhibited caspase-9 activation induced by apoptotic concentrations of $Mn^{2+}$.

Two different groups recently reported that $Zn^{2+}$ can directly inhibit the protease activity of recombinant caspase-3 *in vitro*. Perry *et al*. reported $Zn^{2+}$-mediated inhibition with an $IC_{50}$ of 0.1 $\mu$M whereas Stennicke *et al*. observed a complete inhibition of caspase-3 with 1 mM of $Zn^{2+}$.[20,21] Although it is difficult to compare concentrations of $Zn^{2+}$ available in cells for caspase-3 in our experimental conditions of those described for *in vitro* assays with recombinant caspases, we also observed a similar activity in the presence of high concentrations of $Zn^{2+}$ (from 100 $\mu$M). Indeed, $Zn^{2+}$-mediated caspase-3 activation is associated with the expression of both p19 and p17, the active fragments of caspase-3. However, in contrast to what was observed with $Mn^{2+}$, there was always more p19 than p17 in $Zn^{2+}$-activated Ramos cells (Figure 2 *vs* 4). Since p17 is the autocleavage product of p19, this accumulation of p19 is probably the result of a partial inhibition of the caspase-3 activity by $Zn^{2+}$. Thus, increased $Zn^{2+}$ concentrations should also increase inactivation of caspase-3 activity and lead to the only expression of the p19 form. Unfortunately, in our experimental conditions, concentrations of $Zn^{2+}$ superior to 100 $\mu$M, which should be associated to p19 expression, trigger rapid necrotic death of most cells associated with non specific proteolysis of caspase-3 proform and cleaved fragments (data not shown). Our data suggest that activation of caspase-3 observed in intact cells with $Zn^{2+}$ concentrations from 50 to 100 $\mu$M results probably from a balance between activation of a pathway, including loss of the mitochondrial membrane potential ($\Delta\Psi$m) and caspase-9 activation leading to cleavage and activation of procaspase-3 and a direct inhibition of caspase-3 activity.

Activation of caspase-3 by $Zn^{2+}$ is associated with apoptosis of Ramos cells. This apoptosis presents typical features including cellular events (cell shrinkage and expression of phosphatidylserine residues on the outer leaflet of the cell membrane) and nuclear events (chromatin condensation, DNA cleavage and nuclear fragmentation). This apoptotic process is prevented in the presence of the broad-spectrum caspase inhibitor zVAD-fmk. Such apoptosis is always associated with necrosis which becomes the major cell death process when $Zn^{2+}$ is present at concentrations above 100 $\mu$M and after 48 h of $Zn^{2+}$-activation (data not shown). This raises the question of the interaction between $Zn^{2+}$-mediated apoptotic and necrotic-like death. Vercammen *et al*. recently reported that Fas can activate different pathways leading to apoptosis or necrosis.[38,39] They show that caspase inhibitors block Fas-mediated apoptosis and promote the triggering of a necrotic pathway that involves oxygen radical production. However the dual apoptotic/necrotic death induced by $Zn^{2+}$ seems different from Fas-induced cell death for various reasons: (i) in our conditions, the presence of zVAD-fmk which blocks apoptosis did not affect necrotic cell death within the first 24 h. In contrast, after 48 and 72 h almost all the cells became necrotic and this necrosis was not modified by z-VAD; (ii) we are not able to prevent Ramos cell death in the presence of radical scavengers (data not shown) although superoxide production was associated with an $Zn^{2+}$-activation in as yet poorly characterized caspase-dependent pathway. Thus, $Zn^{2+}$-induced necrotic cells do not result from apoptotic cells because (i) prevention of Ramos cells apoptosis by zVAD-fmk did not prevent the emergence of necrotic cells (in the same way, overexpression of bcl-2 which strongly inhibits apoptosis and also reduced necrosis observed at 24 h does not prevent the massive necrosis observed between 48 and 72 h of activation with $Zn^{2+}$) and (ii) $Zn^{2+}$ can directly trigger caspase-independent necrosis in other B cell types, including other Burkitt cell lines without detectable apoptosis (data not shown).

In conclusion, our data provide the first evidence that $Zn^{2+}$ may regulate caspase-3 activation and apoptosis in Ramos Burkitt lymphoma cells in a dual fashion. Caspase-3 is either inhibited or activated by $Zn^{2+}$ depending on the concentration of cation used and these opposite effects are observed in a narrow range (20 – 100 $\mu$M) of $Zn^{2+}$ concentrations. In view of the increasing therapeutic use of divalent cations, including $Zn^{2+}$ and more recently Arsenic trioxide to treat various diseases,[40,41] our findings point out the importance of a better knowledge of the regulation by divalent cations of different pathways, including caspase activation, controlling cell viability.

# Materials and Methods

## Reagents

Benzyloxycarbonyl-Val-Ala-Asp(OMe)-fluoromethylketone (zVAD-fmk) was purchased from Bachem Biochimie SARL (Voisin le Bretonneux, France). Stock solutions of zVAD-fmk (100 mM) were made in DMSO and kept at $-20^{\circ}$C. The working dilutions were made up freshly immediately prior to use. $ZnCl_2$ and $MnCl_2$ were obtained from Sigma (St. Louis, MO, USA), $DiOC_6(3)$ (3,3′dihexylocarbocyanine iodide) and HE (Hydroethidine) were from Molecular Probes (Interchim, Montluçon, France).

## BL cell lines and bioassays

The Burkitt lymphoma cell line Ramos was obtained from ATCC (Rockville, MD, USA). Ramos cells were negative for the presence of the EBV genome and were cultured in RPMI 1640 Glutamax culture medium (Seromed, Biochrom, Berlin, Germany) supplemented with 100 U/ml penicillin, 100 $\mu$M streptomycin and 5% fetal bovine serum (Gibco, Grand Island, NY, USA) in 24-well flat-bottomed microtest plates (Falcon, Oxnard, CA, USA).

## Cell transfection

The pSFFV-bcl2-neo vector which carries the human bcl-2 cDNA was used to transfect Ramos cells by electroporation. Stable transfectants were isolated and overproduction of Bcl-2 protein by Ramos-bcl-2 cells was verified by flow cytometry using a FITC-labeled anti-human Bcl-2 monoclonal antibody (DAKO A/S, Denmark).

## Determination of cell death and apoptosis.

*Analysis of dot-blot light scatter profiles* Cells ($10^6$) were washed in PBS and resuspended in PBS containing paraformaldehyde (1%). Cells were analyzed for their dot-blot light scatter profiles by flow cytometry using a FACScan flow cytometer (Becton-Dickinson, Mountain View, CA, USA). Apoptotic cells which have a relatively high side-scatter and low forward-scatter properties were enumerated as a percentage of the total population.

*Analysis of mitochondrial transmembrane potential and superoxide anions production* $\Delta\Psi$m was evaluated by staining cells ($10^6$) with 40 nM of $DiOC_6(3)$ (stock solution 1 $\mu$M in Ethanol) for 15 min at 37°C. For the analysis of superoxide generation, cells ($10^6$) were stained with 1 $\mu$M HE (stock solution 500 $\mu$M) for 15 min at 37°C. The fluorescence emitted by cells was analyzed with a FACScan flow cytometer (Becton-Dickinson) using the FL1 channel for $DiOC_6(3)$ and FL2 for HE.

*Hypodiploid DNA* Cells ($10^6$) were washed in PBS and resuspended in 1 ml hypotonic fluorochrome solution (50 $\mu$g ml$^{-1}$ propidium iodide in 0.1% sodium citrate plus 0.1% Triton X-100) (Sigma) as previously described.[42] Samples were placed at room temperature for 1 h before flow-cytometry analysis of PI fluorescence of individual nuclei using a FACScan flow cytometer (Becton-Dickinson). Debris was excluded from analysis by raising the forward scatter threshold. The DNA content of the intact nuclei was registered on a logarithmic scale. Apoptotic cells were identified as the nuclei having hypodiploid DNA emitting fluorescence in channels 10–200 and were enumerated as a percentage of the total population.

*Phosphatidylserine residues expression and loss of cell membrane integrity* Cells ($10^6$) were washed in PBS and resuspended in incubation buffer (10 mM HEPES/NaOH, pH 7.4, 140 mM NaCl, 5 mM $CaCl_2$) with Annexin-V-FITC (Boehringer Mannheim) and 20 $\mu$g/ml propidium iodide (Sigma). After 15 min of incubation at 4°C, the fluorescence emitted by cells was analyzed with a FACScan flow cytometer. Cells with phosphatidylserine residues on the outer leaflet and without loss of cell integrity ($PS^+/PI^-$) were considered as apoptotic cells whereas $PS^+/PI^+$ were considered as necrotic cells and $PS^-/PI^-$ as viable cells.

*Nuclear fragmentation* Cells were collected, washed with PBS and fixed for 10 min in PBS containing 4% paraformaldehyde. After centrifugation, cells were resuspended in PBS containing 1 $\mu$g/ml DAPI. Nuclear morphology was then monitored under a fluorescence microscope (Leica DM RB).

*DNA fragmentation* Cells ($2\times10^6$) were incubated with cations for various periods of time, washed twice in PBS and then lysed with 30 $\mu$l of a buffer containing 10 mM Tris (pH 7.5), 5 mM EDTA, and 0.5% Triton X-100 for 30 min at room temperature. Cell lysates were centrifuged at 15 000 $\times$ *g* for 20 min and the supernatants incubated with proteinase K (0.2 mg/ml) and ribonuclease A (0.1 mg/ml) at 42°C for 1 h. The samples were electrophoresed in a 2% agarose gel in 0.5 $\times$ TBE running buffer (4.5 mM Tris, 4.5 mM boric acid, 62.5 $\mu$M EDTA) containing ethidium bromide (10 $\mu$g/ml).

## Western blotting analysis

Cells were lysed by incubation with modified Laemmli buffer (60 mM Tris, pH 6.8, 10% glycerol, and 2% SDS, without $\beta$-mercaptoethanol and bromophenol blue) and sonication for 30 s on ice. The samples were centrifuged for 5 min at 15 000 $\times$ *g*. The supernatants were boiled for 5 min and frozen at $-80^{\circ}$C or used immediately. Aliquots of the supernatant were assayed for protein concentration (micro-BCA protein assay, Pierce Chemical Co., Rockford, IL, USA). Cell lysate proteins (20 $\mu$g per lane) were resolved by 7.5% and 15% SDS-polyacrylamide gel electrophoresis. Proteins were then electroblotted onto 0.45 $\mu$m pore-size nitrocellulose filters, and the filters were blocked for 1 h with 5% non-fat milk in PBS, 0.1% Tween-20. The filters were then incubated for 1 h at room temperature with anti-caspase-3 Ab (1 $\mu$g ml$^{-1}$) (polyclonal rabbit Anti-Caspase-3 antiserum, Pharmingen, San Diego, CA, USA), anti p37 active cleaved caspase-9 Ab (2 $\mu$g ml$^{-1}$) (polyclonal rabbit Anti-Caspase-9 antiserum, New England Biolabs Inc, Beverly, MA, USA) or PARP mAb C2.10 (1 $\mu$g ml$^{-1}$) (purchased from Dr Poirier, Quebec, Canada). Blots were washed three times for 10 min with 0.2% Tween 20 in PBS and incubated for 1 h with peroxidase-labeled anti-mouse or anti-rabbit immunoglobulins (1/5000). Blots were developed using an enhanced chemiluminescence detection system (ECL, Amersham Corp., UK).

## Detection of active caspase-3 in intact cells

A cell-permeable fluorogenic substrate (Phiphilux-$G_1D_2$) was used to monitor caspase-3 activity in intact cells, according to the manufacturer's recommendations (OncoImmunin, Inc, Kensington, MD,USA). Briefly, after $Zn^{2+}$ stimulation for 8 h, $10^6$ cells were collected and resuspended in 50 $\mu$l of substrate solution and supplemented with 2.5 $\mu$l of fetal calf serum. Cells were incubated in a 5% $CO_2$ incubator at 37°C for 1 h. After incubation, cells were washed once and the fluorescence emission was determined using the FL-1 channel of a FACScan flow cytometer (Becton-Dickinson).

## Acknowledgements

We would like to thank Dr. J Bertoglio for the bcl-2 plasmid. This work was supported by INSERM and grants from Association pour la Recherche sur le Cancer (ARC, Villejuif, France) and Ligue Nationale Contre le Cancer. N Schrantz received a fellowship from MESR (Ministère de l'Enseignement Supérieur et de la Recherche) and FRM (Fondation pour la Recherche Médicale). L Besnault received a fellowship from Association pour la Recherche sur le Cancer (ARC, Villejuif, France).

## References

1. Cuajungco MP and Lees GJ (1997) Zinc metabolism in the brain: relevance to human neurodegenerative disorders. Neurobiol. Dis. 4: 137 – 169
2. Jameson S (1993) Zinc status in pregnancy: the effect of zinc therapy on perinatal mortality, prematurity, and placental ablation. Ann. NY Acad. Sci. 678: 178 – 192
3. Mori H, Matsumoto Y, Tamada Y and Ohashi M (1996) Apoptotic cell death in formation of vesicular skin lesions in patients with acquired zinc deficiency. J. Cutan. Pathol. 23: 359 – 363
4. Neves Jr I, Bertho AL, Veloso VG, Nascimento DV, Campos-Mello DL and Morgado MG (1998) Improvement of the lymphoproliferative immune response and apoptosis inhibition upon in vitro treatment with zinc of peripheral blood mononuclear cells (PBMC) from HIV+ individuals. Clin. Exp. Immunol. 111: 264 – 268
5. Simkin PA (1997) Zinc, again [editorial; comment]. J. Rheumatol. 24: 626 – 628
6. Trubiani O, Antonucci A, Palka G and Di Primio R (1996) Programmed cell death of peripheral myeloid precursor cells in Down patients: effect of zinc therapy. Ultrastruct. Pathol. 20: 457 – 462
7. Baum MK, Shor-Posner G, Lu Y, Rosner B, Sauberlich HE, Fletcher MA, Szapocznik J, Eisdorfer C, Buring JE and Hennekens CH (1995) Micronutrients and HIV-1 disease progression. Aids 9: 1051 – 1056
8. Fraker PJ, Osati-Ashtiani F, Wagner MA and King LE (1995) Possible roles for glucocorticoids and apoptosis in the suppression of lymphopoiesis during zinc deficiency: a review. J. Am. Coll. Nutr. 14: 11 – 17
9. Wellinghausen N, Kirchner H and Rink L (1997) The immunobiology of zinc [see comments]. Immunol. Today 18: 519 – 521
10. Antonucci A, Di Baldassarre A, Di Giacomo F, Stuppia L and Palka G (1997) Detection of apoptosis in peripheral blood cells of 31 subjects affected by Down syndrome before and after zinc therapy. Ultrastruct. Pathol. 21:449 – 452
11. Boukaiba N, Flament C, Acher S, Chappuis P, Piau A, Fusselier M, Dardenne M and Lemonnier D (1993) A physiological amount of zinc supplementation: effects on nutritional, lipid, and thymic status in an elderly population. Am. J. Clin. Nutr. 57:566 – 572
12. Fraker PJ and Telford WG (1997) A reappraisal of the role of zinc in life and death decisions of cells. Proc. Soc. Exp. Biol. Med. 215:229 – 236
13. Decker P, Briand JP, de Murcia G, Pero RW, Isenberg DA and Muller S (1998) Zinc is an essential cofactor for recognition of the DNA binding domain of poly(ADP-ribose) polymerase by antibodies in autoimmune rheumatic and bowel diseases. Arthritis Rheum. 41:918 – 926
14. Karlin S and Zhu ZY (1997) Classification of mononuclear zinc metal sites in protein structures. Proc. Natl. Acad. Sci. U.S.A. 94:14231 – 14236
15. Mahadevan D, Thanki N, Aroca P, McPhie P, Yu JC, Beeler J, Santos E, Wlodawer A and Heidaran MA (1995) A divalent metal ion binding site in the kinase insert domain of the alpha-platelet-derived growth factor receptor regulates its association with SH2 domains. Biochemistry 34:2095 – 2106
16. Vallee BL and Falchuk KH (1993) The biochemical basis of zinc physiology. Physiol. Rev. 73:79 – 118
17. Giannakis C, Forbes IJ and Zalewski PD (1991) Ca2+/Mg(2+)-dependent nuclease: tissue distribution, relationship to inter-nucleosomal DNA fragmentation and inhibition by Zn2+. Biochem. Biophys. Res. Commun. 181:915 – 920
18. Zalewski PD, Forbes IJ and Betts WH (1993) Correlation of apoptosis with change in intracellular labile Zn(II) using zinquin [(2-methyl-8-p-toluenesulphonamido-6-quinolyloxy)acetic acid], a new specific fluorescent probe for Zn(II). Biochem. J. 296:403 – 408
19. Truong-Tran AQ, Ho LH, Chai F and Zalewski PD (2000) Cellular zinc fluxes and the regulation of apoptosis/gene-directed cell death. J. Nutr. 130(5S Suppl):1459S – 1466S
20. Perry DK, Smyth MJ, Stennicke HR, Salvesen GS, Duriez P, Poirier GG, and Hannun YA (1997) Zinc is a potent inhibitor of the apoptotic protease, caspase-3. A novel target for zinc in the inhibition of apoptosis. J. Biol. Chem. 272:18530 – 18533
21. Stennicke HR and Salvesen GS (1997) Biochemical characteristics of caspases-3, -6, -7, and -8. J. Biol. Chem. 272:25719 – 25723
22. Cohen GM (1997) Caspases: the executioners of apoptosis. Biochem. J. 326:1 – 16
23. Fernandes-Alnemri T, Armstrong RC, Krebs J, Srinivasula SM, Wang L, Bullrich F, Fritz LC, Trapani JA, Tomaselli KJ, Litwack G and Alnemri ES (1996) In vitro activation of CPP32 and Mch3 by Mch4, a novel human apoptotic cysteine protease containing two FADD-like domains. Proc. Natl. Acad. Sci. U.S.A. 93:7464 – 7469
24. Slee EA, Harte MT, Kluck RM, Wolf BB, Casiano CA, Newmeyer DD, Wang HG, Reed JC, Nicholson DW, Alnemri ES, Green DR and Martin SJ (1999) Ordering the cytochrome c-initiated caspase cascade: hierarchical activation of caspases-2, -3, -6, -7, -8, and -10 in a caspase-9- dependent manner [In Process Citation]. J. Cell. Biol. 144:281 – 292
25. Anel A, Gamen S, Alava MA, Schmitt-Verhulst AM, Pineiro A and Naval J (1997) Inhibition of CPP32-like proteases prevents granzyme B- and Fas-, but not granzyme A- based cytotoxicity exerted by CTL clones. J. Immunol. 158:1999 – 2006
26. Kuida K, Haydar TF, Kuan CY, Gu Y, Taya C, Karasuyama H, Su MS, Rakic P and Flavell RA (1998) Reduced apoptosis and cytochrome c-mediated caspase activation in mice lacking caspase 9. Cell 94:325 – 337
27. Ohta T, Kinoshita T, Naito M, Nozaki T, Masutani M, Tsuruo T and Miyajima A (1997) Requirement of the caspase-3/CPP32 protease cascade for apoptotic death following cytokine deprivation in hematopoietic cells. J. Biol. Chem. 272:23111 – 23116
28. Schrantz N, Blanchard DA, Auffredou MT, Sharma S, Leca G and Vazquez A (1999) Role of caspases and possible involvement of retinoblastoma protein during TGFbeta-mediated apoptosis of human B lymphocytes. Oncogene 18:3511 – 3519
29. Woo M, Hakem R, Soengas MS, Duncan GS, Shahinian A, Kagi D, Hakem A, McCurrach M, Khoo W, Kaufman SA, Senaldi G, Howard T, Lowe SW and Mak TW (1998) Essential contribution of caspase 3/CPP32 to apoptosis and its associated nuclear changes. Genes Dev. 12:806 – 819
30. Schrantz N, Blanchard DA, Mitenne F, Auffredou MT, Vazquez A and Leca G (1999) Manganese induces apoptosis of human B cells: caspase-dependent cell death blocked by bcl-2. Cell Death Differ. 6:445 – 453
31. Aiuchi T, Mihara S, Nakaya M, Masuda Y, Nakajo S and Nakaya K (1998) Zinc ions prevent processing of caspase-3 during apoptosis induced by geranylgeraniol in HL-60 cells. J. Biochem. 124:300 – 303
32. Zapata JM, Takahashi R, Salvesen GS and Reed JC (1998) Granzyme release and caspase activation in activated human T- lymphocytes. J. Biol. Chem. 273:6916 – 6920
33. Zamzami N, Marchetti P, Castedo M, Decaudin D, Macho A, Hirsch T, Susin SA, Petit PX, Mignotte B and Kroemer G (1995) Sequential reduction of mitochondrial transmembrane potential and generation of reactive oxygen species in early programmed cell death. J. Exp. Med. 182:367 – 377
34. Li P, Nijhawan D, Budihardjo I, Srinivasula SM, Ahmad M, Alnemri ES and Wang X (1997) Cytochrome c and dATP-dependent formation of Apaf-1/caspase-9 complex initiates an apoptotic protease cascade. Cell 91:479 – 489
35. Susin SA, Lorenzo HK, Zamzami N, Marzo I, Snow BE, Brothers GM, Mangion J, Jacotot E, Costantini P, Loeffler M, Larochette N, Goodlett DR, Aebersold R, Siderovski DP, Penninger JM and Kroemer G (1999) Molecular characterization of mitochondrial apoptosis-inducing factor [see comments]. Nature 397:441 – 446
36. Susin SA, Lorenzo HK, Zamzami N, Marzo I, Brenner C, Larochette N, Prevost MC, Alzari PM and Kroemer G (1999) Mitochondrial release of caspase-2 and -9 during the apoptotic process. J. Exp. Med. 189:381 – 394
37. Alnemri ES (1997) Mammalian cell death proteases: a family of highly conserved aspartate specific cysteine proteases. J. Cell. Biochem. 64:33 – 42
38. Vercammen D, Brouckaert G, Denecker G, Van de Craen M, Declercq W, Fiers W and Vandenabeele P (1998) Dual signaling of the Fas receptor: initiation of both apoptotic and necrotic cell death pathways. J. Exp. Med. 188:919 – 930
39. Vercammen D, Beyaert R, Denecker G, Goossens V, Van Loo G, Declercq W, Grooten J, Fiers W and Vandenabelle P. (1998) Inhibition of caspases increases the sensitivity of L929 cells to necrosis mediated by tumor necrosis factor. J. Exp. Med. 187:1477 – 1485

40. Quignon F, De Bels F, Koken M, Feunteun J, Ameisen JC, de The H, Soignet SL, Maslak P, Wang ZG, Jhanwar S, Calleja E, Dardashti LJ, Corso D, DeBlasio A, Gabrilove J, Scheinberg DA, Pandolfi PP and Warrell Jr RP (1998) PML induces a novel caspase-independent death process [see comments]. Complete remission after treatment of acute promyelocytic leukemia with arsenic trioxide [see comments]. Nat. Genet. 20:259 – 265
41. Soignet SL, Maslak P, Wang ZG, Jhanwar S, Calleja E, Dardashti LJ, Corso D, DeBlasio A, Gabrilove J, Scheinberg DA, Pandolfi PP and Warrel Jr RP (1998) Complete remission after treatment of acute promyelocytic leukemia with arsenic trioxide [see comments]. N. Engl. J. Med. 339:1341 – 1348
42. Chaouchi N, Arvanitakis L, Auffredou MT, Blanchard DA, Vazquez A and Sharma S (1995) Characterization of transforming growth factor-beta 1 induced apoptosis in normal human B cells and lymphoma B cell lines. Oncogene 11:1615 – 1622